The Company of **Biologists**

RESEARCH ARTICLE

The chemical compound bubblin induces stomatal mispatterning in *Arabidopsis* by disrupting the intrinsic polarity of stomatal lineage cells

Yumiko Sakai[1], Shigeo S. Sugano[1,2], Takashi Kawase[1], Makoto Shirakawa[1], Yu Imai[1], Yusuke Kawamoto[3], Hiroshi Sugiyama[3,4], Tsuyoshi Nakagawa[5], Ikuko Hara-Nishimura[1] and Tomoo Shimada[1,*]

ABSTRACT

Stem cell polarization is a crucial step in asymmetric cell division, which is a universal system for generating cellular diversity in multicellular organisms. Several conventional genetics studies have attempted to elucidate the mechanisms underlying cell polarization in plants, but it remains largely unknown. In plants, stomata, which are valves for gas exchange, are generated through several rounds of asymmetric divisions. In this study, we identified and characterized a chemical compound that affects stomatal stem cell polarity. High-throughput screening for bioactive molecules identified a pyridine-thiazole derivative, named bubblin, which induced stomatal clustering in *Arabidopsis* epidermis. Bubblin perturbed stomatal asymmetric division, resulting in the generation of two identical daughter cells. Both cells continued to express the stomatal fate determinant SPEECHLESS, and then differentiated into mispatterned stomata. Bubblin-treated cells had a defect in the polarized localization of BREAKING OF ASYMMETRY IN THE STOMATAL LINEAGE (BASL), which is required for asymmetric cell fate determination. Our results suggest that bubblin induces stomatal lineage cells to divide without BASL-dependent pre-mitotic establishment of polarity. Bubblin is a potentially valuable tool for investigating cell polarity establishment in stomatal asymmetric division.

INTRODUCTION

Asymmetric cell division produces two cells with different cell fates, thus ensuring cellular diversity in multicellular organisms (Knoblich, 2008). In plants, because of the immobility of their cells, body development strictly relies on spatial and temporal coordination of asymmetric cell divisions (De Smet and Beeckman, 2011). Stomatal development is considered a model system for investigating plant asymmetric division. Stomata are surrounded by guard cells and act as valves for gas exchange between the plant body and atmosphere (Pillitteri and Dong, 2013).

[1]Department of Botany, Graduate School of Science, Kyoto University, Kyoto 606-8502, Japan. [2]Japan Science and Technology Agency, PRESTO, 4-1-8 Honcho Kawaguchi, Saitama 332-0012, Japan. [3]Department of Chemistry, Graduate School of Science, Kyoto University, Kyoto 606-8502, Japan. [4]Institute for Integrated Cell–Material Science (WPI–iCeMS), Kyoto University, Kyoto 606–8501, Japan. [5]Department of Molecular and Functional Genomics, Center for Integrated Research in Science, Shimane University, Matsue 690-8504, Japan.

*Author for correspondence (tshimada@gr.bot.kyoto-u.ac.jp)

T.S., 0000-0002-2101-1003

Stomata are formed by the postembryonic development of protodermal epidermal cells, and are distributed according to a one-cell spacing rule, with at least one pavement cell between stomata. This stomatal patterning is physiologically important for efficient gas exchange (Dow et al., 2014).

The stomatal lineage originates from an epidermal stem cell that undergoes asymmetric divisions to produce a stomatal precursor cell, called a meristemoid, and a non-stomatal cell, which expands to become a pavement cell (Fig. 1A) (Pillitteri and Dong, 2013). Subsequently, the meristemoid undergoes asymmetric division and eventually differentiates into a guard mother cell (GMC), which divides equally to produce a pair of guard cells. Recent studies have revealed many of the components, including transcription factors, secretory peptides and receptors, that are involved in the regulation of stomatal cell fate transitions and division patterns in *Arabidopsis* (Lau and Bergmann, 2012; Pillitteri and Torii, 2012). Three paralogous basic helix-loop-helix (bHLH) transcription factors, namely SPEECHLESS (SPCH), MUTE and FAMA, regulate distinct steps in development: entry of stomatal lineage, fate transition from meristemoid to GMC, and terminal division to produce guard cells, respectively (MacAlister et al., 2007; Ohashi-Ito and Bergmann, 2006; Pillitteri et al., 2007). These steps are also regulated by positional cues, including secretory peptides such as the positive regulator STOMAGEN and the negative regulators EPIDERMAL PATTERNING FACTOR 1 (EPF1) and EPF2, and the cell-surface receptors TOO MANY MOUTHS (TMM), ERECTA (ER), ER-LIKE1 (ERL1) and ERL2 (Torii, 2012). Conversely, only two polarity factors have been identified to date: BREAKING OF ASYMMETRY IN THE STOMATAL LINEAGE (BASL) (Dong et al., 2009) and POLAR (Pillitteri et al., 2011). In the pre-mitotic stage of a stomatal stem cell, BASL is first observed in the nucleus and subsequently localizes to one side of the cell cortex or periphery. When the cell divides, peripheral BASL is inherited by only one of the daughter cells – the cell that will differentiate into a non-stomatal cell. Although this much is known, it remains unclear how the pre-mitotic cell polarity of the stomatal precursor is established and how it regulates asymmetric cell division.

Chemical genetics offers an alternative approach to circumvent problems of conventional genetics, such as redundancy and lethality (Schreiber, 1998; Stockwell, 2000). Chemical compounds can be applied in limited time and space, and are thus recognized as ideal probes for investigating developmental processes. In plant developmental biology, chemical screenings have identified a series of small molecules that affect root architecture or shoot regeneration (Serrano et al., 2015); however, no molecule has been found that affects asymmetric cell division. Stomatal development occurs in the outermost cell layer, which is easily accessed by externally applied chemicals. This feature makes stomatal

DEVELOPMENT

development an ideal system for investigating asymmetric division via a chemical genetic approach. In this study, we used high-throughput phenotypic screening of a chemical library to identify a small pyridine-thiazole derivative capable of perturbing stomatal patterning. This compound, designated bubblin, affected stomatal asymmetric division, resulting in the generation of two identical daughter cells. Our results suggest that bubblin induces stomatal lineage cells to divide without the establishment of stem cell polarity.

RESULTS

The chemical compound bubblin induces stomatal clustering

A high-throughput screening system for chemical compounds that affect stomatal patterning was established using the *Arabidopsis thaliana* transgenic line E1728 (Gardner et al., 2009) (Fig. S1). The E1728 line has GFP-labeled guard cells, which enabled us to easily detect abnormal stomatal patterning by inspecting cotyledons under a fluorescence stereomicroscope. From a total of 3650 bioactive small molecules in a chemical library (Library of Active Compounds on Arabidopsis) (Zhao et al., 2007), we isolated a pyridine-thiazole derivative, 4-(4-bromophenyl)-2-pyridin-3-yl-1,3-thiazole (Fig. 1B), which affected stomatal patterning. We named the compound bubblin because it induced the formation of bubble-shaped clusters of stomata on the cotyledon (Fig. 1C,D).

On the epidermis of 10-day-old cotyledons of a transgenic plant expressing the plasma membrane marker GFP-LTI6b (Cutler et al., 2000), bubblin induced formation of stomatal clusters in a dose-dependent manner (Fig. 1E-G). When the epidermis was treated with 10 μM bubblin, over 20% of the stomata were found in clusters composed of more than five stomata (Fig. 1H). The stomatal clustering was induced by 1 μM bubblin, but not by 100 nM bubblin (Fig. S2). Thus, the minimum bubblin concentration required to affect stomatal development is in the range of 100 nM to 1 μM. Smaller clusters composed of two or three stomata were generated in mock-treated epidermis. This observation was consistent with a previous report that the sucrose in growth medium induces clustered stomata (Akita et al., 2013).

We next examined the heat stability of bubblin. HPLC analysis revealed that bubblin was not degraded by heat treatment at 90°C for 1 h (Fig. S3A). The heat-treated bubblin retained stomatal cluster-inducing activity (Fig. S3B). Additionally, stomatal clustering was enhanced by longer exposure to bubblin, and cluster formation stopped when the plants were transferred to regular medium (Fig. S4). These results indicate that we can easily manipulate the strength of the bubblin effect by treatment time. Bubblin also induced the formation of stomatal clusters on juvenile leaves (Fig. S5A) and hypocotyls (Fig. S5B), indicating that stomatal clustering was induced by bubblin in a tissue-independent manner. However, bubblin had less effect on hypocotyls than on cotyledons or leaves. Bubblin also affected cells other than stomata: inhibition of seedling growth (Fig. S5C), hypocotyl cell elongation (Fig. S5B) and elongation of cultured tobacco cells (Fig. S5D) were also observed.

Structure-activity relationship analysis of bubblin

Bubblin is composed of three aromatic rings: a pyridine, a thiazole and a bromophenyl ring. Of the five derivatives of bubblin, A1 to A5 (Fig. 2A), only A1, which differs in pyridine ring conjugation, showed bubblin-like stomatal clustering activity (Fig. 2B). By contrast, A2, in which the pyridine ring is replaced by a phenyl ring, showed no stomatal clustering activity, even at 50 μM (Fig. S6). These results indicate that the pyridine ring of bubblin is essential for its activity. Removal of the bromo group from the bromophenyl ring (A3) or substitution of the ring to a methylphenyl ring (A4)
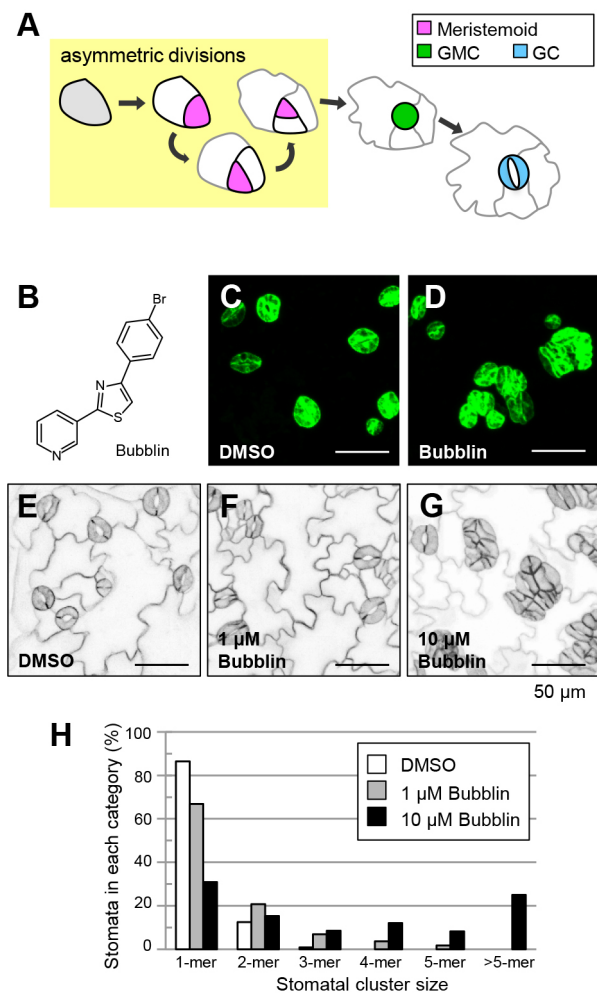

Fig. 1. Bubblin induces the formation of stomatal clusters. (A) Diagram of stomatal development in *Arabidopsis*. The meristemoid is limited to only one daughter cell, which undergoes several rounds of asymmetric divisions. Asymmetric cell fate determination establishes in-spiral epidermal patterning, which is responsible for the stomatal one-cell spacing rule. The meristemoid differentiates into the guard mother cell (GMC) and a pair of guard cells (GCs). (B) Chemical structure of bubblin. (C,D) Confocal images of abaxial cotyledon epidermis from 10-day-old E1728 seedlings treated with DMSO as a control (C) or with 10 μM bubblin (D). (E-G) Confocal images of abaxial cotyledon epidermis from 10-day-old GFP-LTI6b seedlings treated with DMSO (E), 1 μM (F) or 10 μM (G) bubblin. (H) Quantitative analysis of stomatal clustering displayed in E-G. The percentage of stomata in each cluster size class is shown. Stomata (n=636, DMSO; n=864, 1 μM; n=732, 10 μM) from 16 independent observations were counted for each treatment. Bubblin treatments show significant differences compared with DMSO treatment (P<0.001; Fisher's exact test).

reduced stomatal clustering activity, and substitution to a methoxyphenyl ring (A5) resulted in activity loss (Fig. 2B,C, Fig. S6). Accordingly, these results indicate that the bromo group is required for the high activity of bubblin. Compounds with stomatal clustering activity inhibited seedling growth in a dose-dependent manner, whereas compounds without stomatal clustering activity did not inhibit seedling growth (Fig. S7).

A structurally analogous compound, fatostatin (Fig. S8A), was previously identified as an inhibitor of the sterol biosynthesis regulator SCAP (sterol regulatory element-binding protein cleavage-activating protein) in animal cells (Kamisuki et al., 2009). When cotyledons were treated with fatostatin, stomatal clusters did not form, even at 50 μM (Fig. S8B). Additionally,
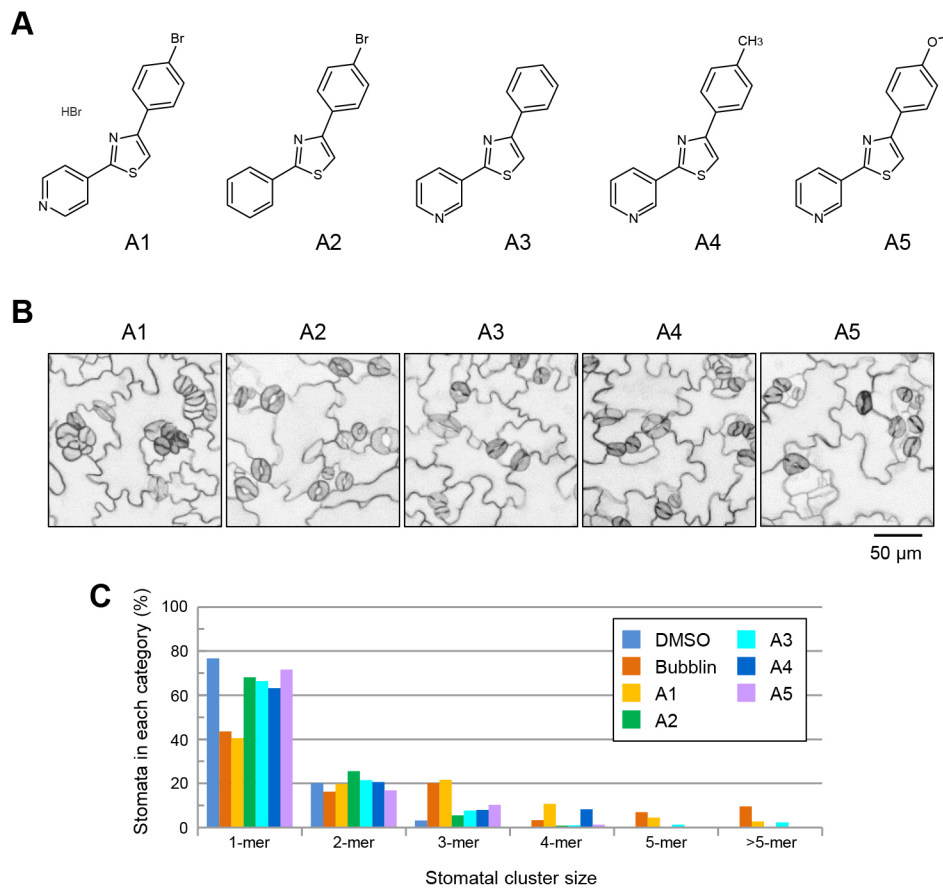
Fig. 2. Five derivatives of bubblin and their effects on stomatal patterning.
(A) Chemical structures of bubblin analogs A1-A5. (B) Confocal images of abaxial cotyledon epidermis from 10-day-old GFP-LTl6b seedlings treated with each compound at 10 μM. (C) Quantitative analysis of stomatal clustering displayed in B. The percentage of stomata in each cluster size class is shown. Stomata (*n*=475, DMSO; *n*=356, bubblin; *n*=222, A1; *n*=486, A2; *n*=392, A3; *n*=339, A4; *n*=320, A5) from ten independent observations were counted for each treatment.

fatostatin had little effect on seedling growth (Fig. S8C). Fatostatin, which has no effect on stomatal development, has a propyl group conjugated to the pyridine ring, whereas A4, which partially induces stomatal clustering, has the same methylphenyl ring structure as fatostatin. These observations revealed that modifying the pyridine ring of bubblin reduces its stomatal clustering activity. Our results suggest that the potency of bubblin is strictly correlated to its structure.

Bubblin treatment produces two daughter cells with the same characteristics

We found that bubblin-treated younger (7-day-old) cotyledons formed excessive numbers of mispatterned (clustered), small, square cells (Fig. S9). To investigate how this patterning occurred, we examined the divisions of stomatal lineage cells over 36 h. During stomatal stem cell asymmetric divisions, one daughter cell retained stem cell activity and underwent subsequent asymmetric divisions, whereas the other typically ceased mitotic division and expanded to become a pavement cell (Fig. 3A, Movies 1-4). By contrast, in bubblin-treated epidermis, both of the daughter cells divided and the integration of these aberrant divisions generated clusters of small cells (Fig. 3B, Movies 5-8).

To quantify this effect of bubblin, we categorized cell divisions into five types according to the fates of the daughter cells. Divisions resulting in two daughter cells with different cell fates were categorized into three types: type 1, stomatal stem cell and pavement cell; type 2, stoma and pavement cell; type 3, stoma and stomatal stem cell. Divisions resulting in two cells differentiating to the same fate were categorized into two types: type 4, stomatal stem cell; type 5, stoma (Fig. S10). Quantitative analysis revealed that bubblin

application increased the occurrence of type 4 divisions over fivefold (Fig. 3C). In bubblin-treated epidermis, over half of the divisions were categorized as type 4 or type 5, resulting in two daughter cells with the same characteristics in stomatal lineage.

Bubblin induces clustered small cells that express stomatal lineage-specific markers

In *Arabidopsis*, three bHLH transcription factor genes, namely *SPCH*, *MUTE* and *FAMA*, are expressed in sequence during stomatal development (Fig. S11A). Using these stomatal-specific markers (*ProSPCH:NUC-GFP*, *ProMUTE:NUC-GFP* and *ProFAMA:VENUS-N7*), we observed that bubblin induced the formation of clusters of small cells that exhibited stomatal lineage activity (Fig. 4A). These observations suggest that bubblin-induced stomatal clusters are formed under the regulation of stomatal-specific bHLH transcription factors. Analysis of endogenous expression levels of stomatal lineage-specific genes also supported ectopic development of stomatal precursors. Quantitative RT-PCR analysis revealed that *SPCH*, *MUTE* and *FAMA* were upregulated after 24 h of bubblin treatment (Fig. 4B), suggesting that bubblin caused the overproliferation of stomatal precursor cells.

Bubblin affects the asymmetric cell divisions in stomatal development

To identify the stage of stomatal development affected by bubblin, we investigated its effects in various genetic backgrounds. Bubblin had no effect on *spch* epidermis, in which no asymmetric divisions occurred and only jigsaw puzzle-shaped epidermal cells were present (Fig. 4C). Similarly, bubblin had no effect on the epidermis
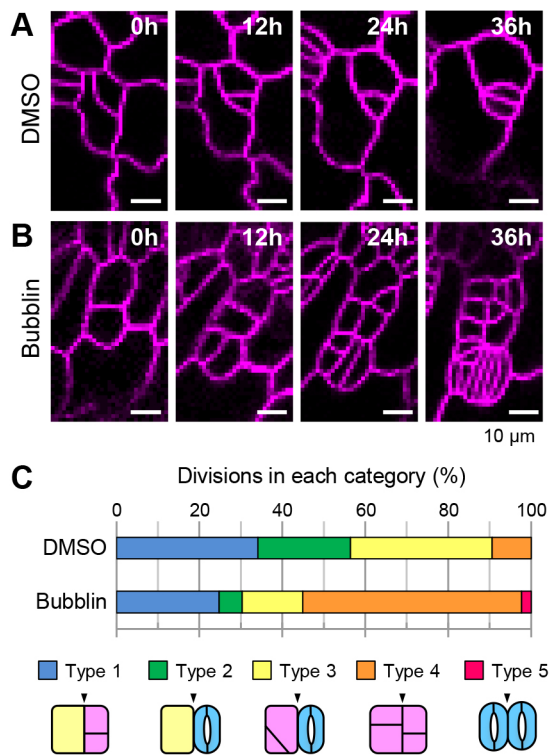
Fig. 3. Bubblin inhibits asymmetric cell fate determination in stomatal stem cells. (A,B) Time-lapse series showing the division pattern of stomatal lineage cells in adaxial cotyledons treated with DMSO (A) or 10 µM bubblin (B). Image acquisition began with 4-day-old seedlings (0 h), and images were acquired at 12-h intervals thereafter. Cell shape was visualized by FM4-64 dye staining (magenta). (C) Quantitative analysis of the effect of bubblin on division as displayed in A and B. Divisions of stomatal stem cells were categorized into five types according to the fates of their daughter cells (see also Fig. S10). Divisions (n=88, DMSO; n=89, bubblin) from five independent cotyledons were counted and the percentage of divisions in each category is shown.

of *EPF2* overexpressors (Fig. S11B). *EPF2* encodes a secretory peptide that represses *SPCH* expression, so the epidermis of *EPF2* overexpressors phenocopies that of *spch*. These results indicate that bubblin acts on stomatal precursors produced by SPCH. By contrast, bubblin application drastically affected *mute* epidermis. The epidermis of *mute* displays arrested triangular meristemoids with inward spiral structures as a consequence of asymmetric divisions. Bubblin-treated *mute* epidermis exhibited overproliferation of meristemoid-like small cells, which lacked the inward spiral structure (Fig. 4D). These observations suggest that bubblin affects stomatal asymmetric divisions and induces disorganized patterning in meristemoids. Similar overproliferation of arrested meristemoids was observed on the epidermis of bubblin-treated *EPF1* overexpressors (Fig. S11B). Overexpression of *EPF1* results in arrested meristemoids and the absence of stomata on the epidermis. *fama* produces stacked narrow cells known as *fama* tumors. When *fama* epidermis was treated with bubblin, both *fama* tumors and bubblin-induced small cell clusters were observed (Fig. 4E). Regarding the *fama* tumors, there were no significant differences in their dividing patterns between bubblin-treated and mock-treated epidermis (Fig. S12). These results were consistent with the idea that bubblin acts at the early stage of stomatal development, i.e. asymmetric cell division.

Asymmetric cell division occurs in various tissues after embryogenesis. One representative example is the asymmetric division of the cortex/endodermis initial cell, which regulates root

radial patterning in *Arabidopsis*. We applied bubblin to the root apical meristem of the endodermis marker line *ProSCR:GFP-γTIP*, but found no evidence of excessive cell layers or abnormal cell divisions (Fig. S13). These observations suggest that bubblin does not affect asymmetric cell division in the root apical meristem.

Bubblin induces stomatal clusters by a different mechanism to *tmm* or stomagen application
Asymmetric cell divisions are regulated by two fundamental mechanisms: intrinsic cell polarity and extrinsic positional cues (Knoblich, 2008). During plant stomatal development, both mechanisms are well orchestrated and determine the distribution of meristemoids (Facette and Smith, 2012). To investigate whether bubblin affects the extrinsic pathway or intrinsic polarity, we first monitored the expression pattern of *STOMATAL DENSITY AND DISTRIBUTION 1* (*SDD1*), a specific marker of GMCs and early guard cells (Fig. 5A) (Von Groll et al., 2002). In bubblin-treated epidermis, *ProSDD1:GFP* signals were observed in adjacent cells that subsequently formed a stomatal cluster (Fig. 5B). By contrast, when we applied stomagen, an extrinsic positive regulator of stomatal development, *ProSDD1:GFP* signals were observed in non-adjacent cells (Fig. 5C, Fig. S14A). Further analysis revealed that *ProSDD1:GFP* signals were present in a GMC or a pair of guard cells that were often adjacent to other stomatal lineage cells, such as meristemoids or mature guard cells, in stomagen-treated epidermis. These observations suggest that bubblin and stomagen cause stomatal clustering by different mechanisms. Additionally, in *tmm* epidermis, which has defects in the extrinsic signaling pathway involving stomagen (Lee et al., 2015), *ProSDD1:GFP*-positive cells were not attached to each other (Fig. 5D). These different expression profiles of *ProSDD1:GFP* suggest that bubblin affects a pathway that is independent of the extrinsic cell-to-cell signaling pathway involving stomagen and TMM (Fig. S14B).

Bubblin abolishes intrinsic polarity in stomatal lineage cells
Stomatal asymmetric divisions are accompanied by asymmetric degradation of SPCH, a stomatal lineage determinant, after cell division (Robinson et al., 2011). SPCH is expressed in both daughter cells after cytokinesis, but is immediately degraded in one cell, which subsequently grows in size to form a pavement cell. In mock-treated epidermis, SPCH-GFP signals were observed in a pair of cells and a single cell after division (Fig. 5E). By contrast, in bubblin-treated epidermis, SPCH-GFP signals were observed in attached small cells, suggesting that SPCH remained in daughter cells following cell divisions (Fig. 5F).

Recently, SPCH degradation was suggested to be regulated by the polarity factor BASL, which is specifically localized at the cell periphery (Zhang et al., 2015). In the pre-mitotic stomatal precursor cell, BASL is observed in the nucleus and at the cell periphery. After cell division, nuclear BASL is seen in both daughter cells, but peripherally localized BASL is maintained in only one of the daughter cells (Fig. S15A, Movie 9) (Dong et al., 2009). Thus, the peripheral BASL determines the polarity of the stomatal stem cell. In bubblin-treated epidermis, BASL was localized to the nuclei of the clustered small cells but did not exhibit polar localization at the periphery (Fig. S15B, Movies 10 and 11). To quantify this effect of bubblin, we examined cell pairs expressing nuclear BASL and assessed whether they maintained peripheral BASL (Fig. 5G). Bubblin application drastically increased the proportion of cell divisions without peripheral BASL. These results suggest that bubblin disrupts pre-mitotic cell polarity in stomatal lineage cells to produce stomatal clusters. *BASL*-deficient mutants have also been
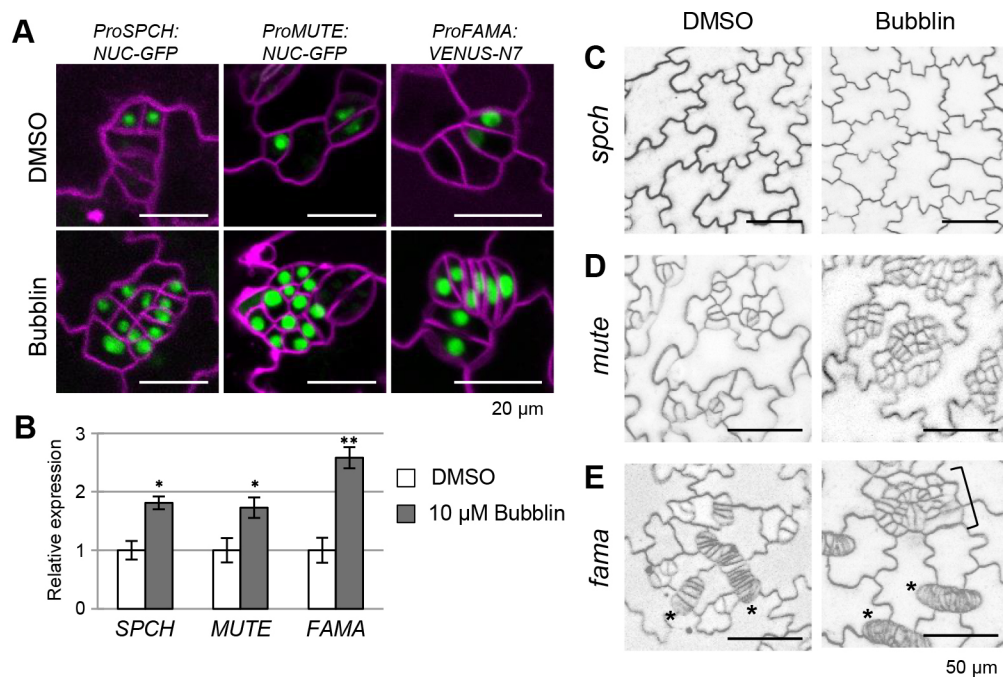
Fig. 4. Bubblin affects asymmetric cell divisions and induces disorganized patterning in stomatal precursor cells. (A) Confocal images of adaxial cotyledon epidermis from 7-day-old *ProSPCH:NUC-GFP*, *ProMUTE:NUC-GFP* and *ProFAMA:VENUS-N7* seedlings treated with DMSO or 10 μM bubblin. Cell shape was visualized by FM4-64 dye staining (magenta); GFP or VENUS is in green. (B) Quantitative RT-PCR using total RNA from aerial tissue of 4-day-old wild-type seedlings treated with DMSO or 10 μM bubblin for 24 h. Mean±s.d. from three independent experiments. Student's *t*-test, *$P<0.01$, **$P<0.001$. (C-E) Confocal images of adaxial cotyledon epidermis from 7-day-old *spch* (C), 10-day-old *mute* (D) and abaxial cotyledon epidermis from 7-day-old *fama* (E). Epidermal structures treated with DMSO (left) or 10 μM bubblin (right) are shown. Cell shape was visualized by FM4-64 dye staining. Bubblin-induced small cell clusters (bracket) and *fama* tumors (asterisks) are indicated.

shown to exhibit stomatal clusters (Dong et al., 2009). We found that bubblin enhanced the stomatal clustering phenotype in *basl* mutants (Fig. S16). These results suggest that bubblin affects one or more factors other than BASL that regulate stomatal patterning, although the possibility that bubblin could directly inhibit peripheral BASL accumulation is not excluded.

DISCUSSION
Asymmetric division is a fundamental mechanism to generate cellular diversity. To our knowledge, this is the first study in which a large-scale chemical library has been screened to isolate compounds affecting asymmetric division in stomatal patterning. We established a high-throughput screening system using intact *Arabidopsis* seedlings that identified bubblin as a stomatal clustering molecule. Bubblin, or a product of its metabolism, perturbed stomatal asymmetric division and induced the formation of mispatterned stomatal precursors. Bubblin affected cell elongation throughout *Arabidopsis* seedlings and in cultured tobacco cells, but showed no effects on asymmetric division in root apical meristem. From these data, we hypothesize that bubblin has a dual effect on cell elongation and stomatal asymmetric cell division.

Stomatal clusters are also generated in *TMM*-deficient mutants or by excessive application of stomagen (Sugano et al., 2010; Yang and Sack, 1995); however, in this study we revealed that GMC clusters are rarely formed in these cases. These observations are consistent with previous reports that extrinsic signals in stomatal development mainly regulate the number of stem cells and the orientation of their divisions, but not intrinsic cell polarity (Geisler et al., 2000). By contrast, bubblin abolishes the asymmetry of cell division and causes stomatal precursor clustering, suggesting that bubblin acts on cell polarity independently of extrinsic signaling. Meristemoid cell

polarity is generated by BASL that localizes to the cell periphery and is predicted to regulate SPCH degradation (Zhang et al., 2015). Bubblin induced stomatal lineage cells to divide without establishing BASL polarity, and this accounted for the retention of SPCH, which resulted in stomatal clustering (Fig. 5H). Our results suggest that a possible target of bubblin is involved in regulating stem cell polarity establishment prior to cell division in stomatal development.

To achieve successful asymmetric cell division, cell polarity establishment and cell cycle progression must be tightly coupled. In animals, polarized cells only divide after polarity is fully established, so that polarized elements are correctly segregated into the daughter cells (Noatynska et al., 2013). In stomatal lineage cells, however, how the cell cycle is coordinated with specific cell polarity factors has not been clarified. Robinson et al. (2011) suggested that the re-establishment of peripherally localized BASL is essential for achieving the stomatal one-cell spacing pattern. Our findings suggest that bubblin acts on the fine-tuned coordination between the re-establishment of peripheral BASL and cell cycle progression in stomatal lineage cells. One possible mode of action of bubblin is that it accelerates cell division in meristemoids, even in the absence of cell polarity, by abolishing the activity of some negative regulator of the cell cycle. Our time-lapse analysis supports this idea because stomatal lineage cells treated with bubblin divided more often than control cells: bubblin-treated cells underwent three rounds of asymmetric division in 36 h (Fig. 3B), whereas asymmetric division occurred only once in control cells (Fig. 3A). *Arabidopsis* broadly expresses a protein called RETINOBLASTOMA-RELATED (RBR), which restricts cell cycle progression (Gutzat et al., 2012). Reducing RBR function results in excessive division of stomatal lineage cells at both early and terminal stages (Borghi et al., 2010; Lee et al., 2014; Matos
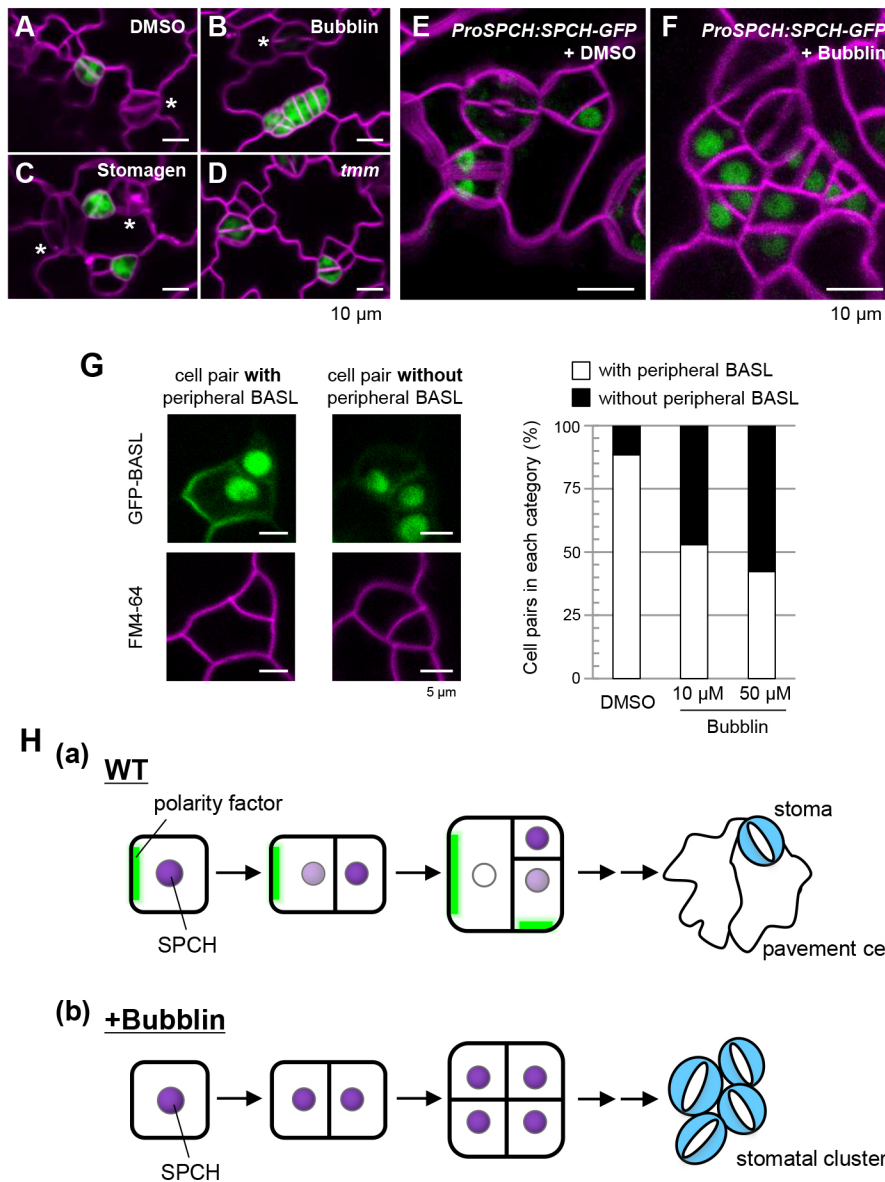
Fig. 5. Bubblin affects stomatal patterning through intrinsic cell polarity rather than extrinsic cell-to-cell signaling pathways. (A-C) Confocal images of adaxial cotyledon epidermis from 6-day-old *ProSDD1:GFP* seedlings treated with DMSO (A), 10 µM bubblin (B) or 10 µM stomagen (C). Mature stomata are indicated by asterisks. (D) Confocal image of adaxial cotyledon epidermis from 6-day-old *tmm* seedling expressing *ProSDD1:GFP*. (E,F) Confocal images of adaxial cotyledon epidermis from 7-day-old *ProSPCH: SPCH-GFP* seedlings treated with DMSO or 10 µM bubblin. (G) (Left) Confocal images of adaxial cotyledon epidermis from *ProBASL:GFP-BASL* seedlings. Cell pairs expressing nuclear BASL were divided into two groups according to whether they maintained peripheral BASL. (Right) The proportion of cell divisions with or without peripheral BASL in epidermis treated with DMSO, 10 µM bubblin or 50 µM bubblin. Cell pairs (*n*=87, DMSO; *n*=70, 10 µM bubblin; *n*=194, 50 µM bubblin) from six independent plants were counted for each treatment. Cell shape was visualized by FM4-64 dye staining (magenta) in all confocal images in this figure. (H) Model of bubblin-induced inhibition of asymmetric cell fate determination during stomatal development. (a) In wild type, at the pre-mitotic stage of a stomatal precursor, polarity factors (green) including BASL are localized to the cell periphery. After cell division, the polarity factors are inherited by only one of the daughter cells and promote the degradation of SPCH in the nucleus (violet). The cell that loses SPCH differentiates into a pavement cell, whereas the cell with SPCH retains stomatal lineage activity. (b) Bubblin causes stomatal clustering by inhibiting cell polarity establishment. Bubblin induces stomatal lineage cells to divide without establishing polarity, which inhibits the asymmetric degradation of SPCH.

et al., 2014). Bubblin affects early stomatal lineage cells that undergo asymmetric divisions; however, it has little effect on mature guard cells. Hence, bubblin appears not to act on RBR itself, but on cell cycle regulators that function in a narrower range of stomatal development.

Another possibility is that bubblin inhibits polarity factors, including BASL. Peripheral localization of BASL requires MPK3/6-mediated phosphorylation (Zhang et al., 2015). Bubblin might act as a kinase inhibitor to perturb BASL phosphorylation or regulate the targeting of phosphorylated BASL to the cell periphery. Bubblin abolished the peripheral accumulation of BASL in stomatal lineage cells, but still enhanced the stomatal clustering phenotype when it was applied to *basl* mutants (Fig. 5G, Fig. S16). Previous reports suggest that an alternative mechanism, acting in parallel to the BASL pathway, regulates stomatal stem cell polarity because the stomatal clustering defects in *basl* mutants are milder than those observed in transformants with defects in SPCH degradation (Lampard et al., 2008; Zhang et al., 2015). Bubblin might inhibit the multiple determinants of cell polarity by affecting protein accumulation at the periphery of stomatal cells.

At present, any direct target of bubblin and its inhibitory mechanism remain unknown. Previous studies in animals show that some pyridine-thiazole molecules exhibit bioactivity by binding to their target proteins. Fatostatin directly interacts with the endoplasmic reticulum (ER)-localized protein SCAP and inhibits the ER-Golgi translocation of sterol regulatory element-binding proteins (SREBPs) (Kamisuki et al., 2009). Pyridine-thiazole analogs of resveratrol bind to the active site of aromatase, an estrogen synthase (Mayhoub et al., 2012). Bubblin might interact with a target protein, either membrane-bound or soluble, and perturb its enzymatic activity or capacity to engage in protein-protein interactions.

Although it is important to establish cell polarity prior to asymmetric division, there are few studies to support this event in plant development. Recently, there have been a number of reports on the use of chemical probes to investigate plant development (Serrano et al., 2015); however, no molecule had been found that affects stem cell polarity. Bubblin is the first chemical tool for investigating asymmetric division and cell polarity in plants. Furthermore, bubblin caused stomatal lineage cells to divide

symmetrically, generating two cells with stomatal cell fates. The spatiotemporal application of bubblin enables us to artificially direct stomatal stem cells to divide symmetrically, and to regulate the number of stomatal precursors. Bubblin is a potentially valuable tool for clarifying the mechanism underlying cell polarity establishment during asymmetric cell division in plants.

MATERIALS AND METHODS
Chemical library and screens
We screened the 96-well format chemical library LATCA (Library of Active Compounds on Arabidopsis) (Zhao et al., 2007). This library was assembled from three commercial libraries: Diverset (ChemBridge), LOPAC (Sigma-Aldrich) and Spectrum (Microsource Discovery Systems). The LATCA library consists of 3650 small molecules and all compounds were dissolved in dimethyl sulfoxide (DMSO) at 2.5 or 5 mM. For screening, each chemical compound was added at 1:255 dilution to liquid medium containing 1% (w/v) sucrose and Murashige and Skoog (MS) salts (Wako) and incubated with a few E1728 seeds (Gardner et al., 2009). Black-well plates and cotton balls in each well helped E1728 seedlings to grow straight, enabling easy observation of whole cotyledons. After incubation at 22°C for 7 or 8 days, stomatal patterning in cotyledons was observed under an Olympus MVX10 fluorescence stereomicroscope.

Bubblin and other chemical compounds
Bubblin [4-(4-bromophenyl)-2-pyridin-3-yl-1,3-thiazole] was purchased from Key Organics (MS-6628). Additional analogous compounds were obtained from other sources: A1 [4-(4-bromophenyl)-2-pyridin-4-yl-1,3-thiazole;hydrobromide] from Maybridge (ML00034); A2 [4-(4-bromophenyl)-2-phenyl-1,3-thiazole] and A5 [4-(4-methoxyphenyl)-2-pyridin-3-yl-1,3-thiazole] from ENAMINE (Z48854171 and Z48847277); A3 (4-phenyl-2-pyridin-3-yl-1,3-thiazole) from Alfa Aesar (H51748); A4 [4-(4-methylphenyl)-2-pyridin-3-yl-1,3-thiazole] from Vitas-M Laboratories (STK723938); and fatostatin hydrobromide from Sigma-Aldrich (F8932).

Heat treatment and HPLC analysis
Bubblin was dissolved in DMSO (Nacalai Tesque) at 10 mM and incubated at 22°C or 90°C for 1 h, then these samples were diluted 1:10 in DMSO and subjected to HPLC. The HPLC analysis was performed on a PU-2089 Plus series system (JASCO) using a CHEMCOBOND 4.6 mm×150 mm 5-ODS-H column (Chemco Plus Scientific) in 0.1% (v/v) trifluoroacetic acid in water, with a linear elution gradient of 0-100% acetonitrile at a flow rate of 1.0 ml/min for 20 min with detection at 254 nm.

Plant materials
Arabidopsis thaliana Columbia-0 (Col-0, CS60000) ecotype was used as wild type except for *mute-2* where Ws-4 was used. T-DNA insertion mutants and an enhancer trap line were obtained from the following sources: SAIL_36_B06 (*spch-3*), SALK_100073 (*fama-1*) and SALK_011958 (*tmm*) from the Arabidopsis Biological Resource Center (ABRC) at Ohio State University; FLAG_225D03 (*mute-2*) from the French National Institute for Agricultural Research (INRA); and E1728 from the Nottingham Arabidopsis Stock Centre (NASC). Transgenic plants used were: *Pro35S:GFP-LTI6b* (Cutler et al., 2000) and *ProSCR:GFP-γTIP* (Saito et al., 2005). Seeds of *SPCH:SPCH-GFP* (*ProSPCH:SPCH-GFP*), *SPCH:nucGFP* (*ProSPCH:NUC-GFP*), *MUTE:nucGFP* (*ProMUTE: NUC-GFP*), *BASL:GFP-BASL* (*ProBASL:GFP-BASL*) and *basl-2* were kindly provided by Dominique C. Bergmann (Stanford University). The Gateway cloning system (Life Technologies) was used to construct *pGWB1 ProFAMA:VENUS-N7*, *pB2GW7 Pro35S:EPF1*, *pB2GW7 Pro35S:EPF2* and *pGWB250 ProSDD1:GFP*. The sequence of *VENUS* fused to *N7* was amplified by PCR using primers 5′-CAAAGGGTGGGCGCGATGGTG-AGCAAGGGCGAG-3′ and 5′-AGCTGGGTCGGCGCGTTACTCTTCT-TCTTGATC-3′ from a *VENUS-N7* sequence cloned in *Pro35S:DII-VENUS-N7* (Brunoud et al., 2012). The In-Fusion HD Cloning Kit (Takara Bio) was used to introduce the DNA sequence of *VENUS-N7* into the *Asc*I site of the pENTR/D-TOPO FAMApro plasmid (Shirakawa et al., 2014). The pENTR/D-TOPO ProFAMA:VENUS-N7 plasmid was

introduced into the binary vector pGWB1 (Nakagawa et al., 2007) using the LR reaction. The coding regions of *EPF1* and *EPF2* were amplified by PCR using primers 5′-CACCATGAAGTCTCTTCTTCTCCTT-3′ and 5′-GCTTATTTCCTTTCAAGGGACAGGGTAGGA-3′ for *EPF1*; and 5′-CACCATGACGAAGTTTGTACGCAA-3′ and 5′-GGGCCAATAGC-ATTTAATTTAATATCCC-3′ for *EPF2*. These fragments were cloned into pENTR/D-TOPO and introduced into pB2GW7 (Karimi et al., 2002) using LR reactions. The promoter region of *SDD1* spanning −2039 bp to +3 bp relative to the start codon (+1) was prepared by PCR with primers 5′-CACCATGGGGTGAGCTGTGTG-3′ and 5′-CATTGGAGAGAGTTAA-AAAAAGGAG-3′. The amplified fragment was cloned into pENTR/D-TOPO to produce pENTR/D-TOPO ProSDD1. Then, the plasmid was subjected to the LR reaction with the destination vector pGWB250 (Keerthisinghe et al., 2015). The constructs were introduced into plants using *Agrobacterium tumefaciens*-mediated transformation via the floral-dip method (Clough and Bent, 1998). Plants expressing *ProSDD1:GFP* were crossed with *tmm* to observe *ProSDD1:GFP* patterning in the *tmm* background. The genotype of this line was confirmed by PCR amplification using the gene-specific primers 5′-GGGCATGTGCTTTTCGTATGCACA-GAC-3′ and 5′-AAAGACTTGGAAGTGCTTGACACG-3′, and the T-DNA-specific primer 5′-TGGTTCACGTAGTGGGCCATCG-3′.

Plant growth conditions and chemical treatments
Seeds were surface-sterilized with 70% ethanol and then sown onto 0.5% (w/v) gellan gum (Wako) containing 1% (w/v) sucrose and MS salts. The seeds were incubated at 22°C under continuous light, and then transferred onto vermiculite for growth in 16 h light/8 h dark cycles at 22°C. In chemical assays, sterilized seeds were sown onto solid medium as described above and incubated at 4°C for 2-3 days to break seed dormancy. Then, the seeds were transferred into liquid MS medium containing 1% (w/v) sucrose with 0.2% (v/v) DMSO or each compound dissolved in DMSO, and were germinated and grown for the indicated days under continuous light at 22°C.

Suspension cultured cells of tobacco BY-2 (*Nicotiana tabacum* L. cv. Bright Yellow 2) were maintained as described previously (Mitsuhashi et al., 2000). BY-2 cells were subcultured in MS medium once a week at 26°C in the dark with an orbital shaker. For chemical assays, 2-day-old BY-2 culture was diluted 1:2 in MS medium and co-incubated with 0.01% (v/v) DMSO or bubblin dissolved in DMSO for 3 days.

Confocal laser scanning microscopy
Confocal images were obtained using a Zeiss LSM 780 laser scanning microscope equipped with a 488 nm 40 mW Ar/Kr laser or a 544 nm 1 mW He/Ne laser, and a 40×0.95 N.A. or 20×0.80 N.A. dry objective (Plan-Apochromat, 440654-9902-000 or 440640-9902-000, Zeiss). Outlines of cells were visualized by staining with 0.5 mM FM4-64 or 50 μg/ml propidium iodide (PI) as necessary.

Images were analyzed with ZEN2010 software (Zeiss) and processed with ImageJ software (NIH). We extracted the leaf epidermis from stacked images to show epidermal structure at low magnification. Images were scanned from top to bottom (along the z-axis), and the signal intensity at each voxel was compared with a specified threshold intensity. If the intensity of the voxel exceeded the manually determined threshold, we discriminated that the surface was located in the voxel. We extracted voxels in a manually determined range further from the surface. To generate the final 2D images of the leaf epidermis, the extracted regions were processed using maximum intensity projection along the z-axis.

RNA extraction and quantitative RT-PCR
Sterilized wild-type seeds were sown onto solid medium as described above and incubated at 22°C. Then, 3-day-old germinated seeds were transferred into liquid MS medium with 0.2% (v/v) DMSO or 10 μM bubblin dissolved in DMSO. After 24 h, total RNA was isolated from aerial tissue of seedlings using the RNeasy Plant Mini Kit (Qiagen). Total RNA was used to synthesize cDNA with Ready-To-Go RT-PCR beads (GE Healthcare) and oligo(dT)$_{12-18}$ primer (Invitrogen). Quantitative real-time PCR (RT-PCR) was performed with gene-specific primer sets (*SPCH*, At02321069_m1; *MUTE*, At02235996_g1; *FAMA*, At02279294_g1; *ACTIN2*, At02335270_gH; Applied Biosystems) and a TaqMan gene

expression assay kit (Applied Biosystems) with a StepOnePlus RT-PCR system (Applied Biosystems). The relative quantity of target cDNA was calculated using *ACTIN2* as a control.

Author contributions
Y.S., S.S.S., I.H-.N. and T.S. designed the research. Y.S. and S.S.S. performed the chemical screen. Y.S. performed chemical analysis on plants and image analysis. T.K. developed the algorithm for extraction of the leaf epidermis. Y.S., M.S., Y.I. and T.N. generated the transgenic plants. Y.K. and H.S. performed HPLC analysis. Y.S., S.S.S., I.H-.N. and T.S. wrote the manuscript. I.H-.N. and T.S. supervised the study.

Supplementary information
Supplementary information available online at
http://dev.biologists.org/lookup/doi/10.1242/dev.145458.supplemental

References
Akita, K., Hasezawa, S. and Higaki, T. (2013). Breaking of plant stomatal one-cell-spacing rule by sugar solution immersion. *PLoS ONE* **8**, e72456.

Borghi, L., Gutzat, R., Fütterer, J., Laizet, Y., Hennig, L. and Gruissem, W. (2010). *Arabidopsis* RETINOBLASTOMA-RELATED is required for stem cell maintenance, cell differentiation, and lateral organ production. *Plant Cell* **22**, 1792-1811.

Brunoud, G., Wells, D. M., Oliva, M., Larrieu, A., Mirabet, V., Burrow, A. H., Beeckman, T., Kepinski, S., Traas, J., Bennett, M. J. et al. (2012). A novel sensor to map auxin response and distribution at high spatio-temporal resolution. *Nature* **482**, 103-106.

Clough, S. J. and Bent, A. F. (1998). Floral dip: a simplified method for *Agrobacterium*-mediated transformation of *Arabidopsis thaliana*. *Plant J.* **16**, 735-743.

Cutler, S. R., Ehrhardt, D. W., Griffitts, J. S. and Somerville, C. R. (2000). Random GFP::cDNA fusions enable visualization of subcellular structures in cells of *Arabidopsis* at a high frequency. *Proc. Natl. Acad. Sci. USA* **97**, 3718-3723.

De Smet, I. and Beeckman, T. (2011). Asymmetric cell division in land plants and algae: the driving force for differentiation. *Nat. Rev. Mol. Cell Biol.* **12**, 177-188.

Dong, J., MacAlister, C. A. and Bergmann, D. C. (2009). BASL controls asymmetric cell division in *Arabidopsis*. *Cell* **137**, 1320-1330.

Dow, G. J., Berry, J. A. and Bergmann, D. C. (2014). The physiological importance of developmental mechanisms that enforce proper stomatal spacing in *Arabidopsis thaliana*. *New Phytol.* **201**, 1205-1217.

Facette, M. R. and Smith, L. G. (2012). Division polarity in developing stomata. *Curr. Opin. Plant Biol.* **15**, 585-592.

Gardner, M. J., Baker, A. J., Assie, J.-M., Poethig, R. S., Haseloff, J. P. and Webb, A. A. R. (2009). *GAL4 GFP* enhancer trap lines for analysis of stomatal guard cell development and gene expression. *J. Exp. Bot.* **60**, 213-226.

Geisler, M., Nadeau, J. and Sack, F. D. (2000). Oriented asymmetric divisions that generate the stomatal spacing pattern in Arabidopsis are disrupted by the *too many mouths* mutation. *Plant Cell* **12**, 2075-2086.

Gutzat, R., Borghi, L. and Gruissem, W. (2012). Emerging roles of RETINOBLASTOMA-RELATED proteins in evolution and plant development. *Trends Plant Sci.* **17**, 139-148.

Kamisuki, S., Mao, Q., Abu-Elheiga, L., Gu, Z., Kugimiya, A., Kwon, Y., Shinohara, T., Kawazoe, Y., Sato, S.-i., Asakura, K. et al. (2009). A small molecule that blocks fat synthesis by inhibiting the activation of SREBP. *Chem. Biol.* **16**, 882-892.

Karimi, M., Inzé, D. and Depicker, A. (2002). GATEWAY vectors for *Agrobacterium*-mediated plant transformation. *Trends Plant Sci.* **7**, 193-195.

Keerthisinghe, S., Nadeau, J. A., Lucas, J. R., Nakagawa, T. and Sack, F. D. (2015). The Arabidopsis leucine-rich repeat receptor-like kinase MUSTACHES enforces stomatal bilateral symmetry in Arabidopsis. *Plant J.* **81**, 684-694.

Knoblich, J. A. (2008). Mechanisms of asymmetric stem cell division. *Cell* **132**, 583-597.

Lampard, G. R., MacAlister, C. A. and Bergmann, D. C. (2008). Arabidopsis stomatal initiation is controlled by MAPK-mediated regulation of the bHLH SPEECHLESS. *Science* **322**, 1113-1116.

Lau, O. S. and Bergmann, D. C. (2012). Stomatal development: a plant's perspective on cell polarity, cell fate transitions and intercellular communication. *Development* **139**, 3683-3692.

Lee, E., Lucas, J. R. and Sack, F. D. (2014). Deep functional redundancy between FAMA and FOUR LIPS in stomatal development. *Plant J.* **78**, 555-565.

Lee, J. S., Hnilova, M., Maes, M., Lin, Y.-C. L., Putarjunan, A., Han, S.-K., Avila, J. and Torii, K. U. (2015). Competitive binding of antagonistic peptides fine-tunes stomatal patterning. *Nature* **522**, 439-443.

MacAlister, C. A., Ohashi-Ito, K. and Bergmann, D. C. (2007). Transcription factor control of asymmetric cell divisions that establish the stomatal lineage. *Nature* **445**, 537-540.

Matos, J. L., Lau, O. S., Hachez, C., Cruz-Ramirez, A., Scheres, B. and Bergmann, D. C. (2014). Irreversible fate commitment in the *Arabidopsis* stomatal lineage requires a FAMA and RETINOBLASTOMA-RELATED module. *Elife* **3**, doi: 10.7554/eLife.03271.

Mayhoub, A. S., Marler, L., Kondratyuk, T. P., Park, E.-J., Pezzuto, J. M. and Cushman, M. (2012). Optimization of the aromatase inhibitory activities of pyridylthiazole analogues of resveratrol. *Bioorg. Med. Chem.* **20**, 2427-2434.

Mitsuhashi, N., Shimada, T., Mano, S., Nishimura, M. and Hara-Nishimura, I. (2000). Characterization of organelles in the vacuolar-sorting pathway by visualization with GFP in tobacco BY-2 cells. *Plant Cell Physiol.* **41**, 993-1001.

Nakagawa, T., Kurose, T., Hino, T., Tanaka, K., Kawamukai, M., Niwa, Y., Toyooka, K., Matsuoka, K., Jinbo, T. and Kimura, T. (2007). Development of series of gateway binary vectors, pGWBs, for realizing efficient construction of fusion genes for plant transformation. *J. Biosci. Bioeng.* **104**, 34-41.

Noatynska, A., Tavernier, N., Gotta, M. and Pintard, L. (2013). Coordinating cell polarity and cell cycle progression: what can we learn from flies and worms? *Open Biol.* **3**, 130083.

Ohashi-Ito, K. and Bergmann, D. C. (2006). *Arabidopsis* FAMA controls the final proliferation/differentiation switch during stomatal development. *Plant Cell* **18**, 2493-2505.

Pillitteri, L. J. and Dong, J. (2013). Stomatal development in Arabidopsis. *Arabidopsis Book* **11**, e0162.

Pillitteri, L. J. and Torii, K. U. (2012). Mechanisms of stomatal development. *Annu. Rev. Plant Biol.* **63**, 591-614.

Pillitteri, L. J., Sloan, D. B., Bogenschutz, N. L. and Torii, K. U. (2007). Termination of asymmetric cell division and differentiation of stomata. *Nature* **445**, 501-505.

Pillitteri, L. J., Peterson, K. M., Horst, R. J. and Torii, K. U. (2011). Molecular profiling of stomatal meristemoids reveals new component of asymmetric cell division and commonalities among stem cell populations in *Arabidopsis*. *Plant Cell* **23**, 3260-3275.

Robinson, S., Barbier de Reuille, P., Chan, J., Bergmann, D., Prusinkiewicz, P. and Coen, E. (2011). Generation of spatial patterns through cell polarity switching. *Science* **333**, 1436-1440.

Saito, C., Morita, M. T., Kato, T. and Tasaka, M. (2005). Amyloplasts and vacuolar membrane dynamics in the living graviperceptive cell of the Arabidopsis inflorescence stem. *Plant Cell* **17**, 548-558.

Schreiber, S. L. (1998). Chemical genetics resulting from a passion for synthetic organic chemistry. *Bioorg. Med. Chem.* **6**, 1127-1152.

Serrano, M., Kombrink, E. and Meesters, C. (2015). Considerations for designing chemical screening strategies in plant biology. *Front. Plant Sci.* **6**, 131.

Shirakawa, M., Ueda, H., Nagano, A. J., Shimada, T., Kohchi, T. and Hara-Nishimura, I. (2014). FAMA is an essential component for the differentiation of two distinct cell types, myrosin cells and guard cells, in *Arabidopsis*. *Plant Cell* **26**, 4039-4052.

Stockwell, B. R. (2000). Chemical genetics: ligand-based discovery of gene function. *Nat. Rev. Genet.* **1**, 116-125.

Sugano, S. S., Shimada, T., Imai, Y., Okawa, K., Tamai, A., Mori, M. and Hara-Nishimura, I. (2010). Stomagen positively regulates stomatal density in *Arabidopsis*. *Nature* **463**, 241-244.

Torii, K. U. (2012). Mix-and-match: ligand-receptor pairs in stomatal development and beyond. *Trends Plant Sci.* **17**, 711-719.

Von Groll, U., Berger, D. and Altmann, T. (2002). The subtilisin-like serine protease SDD1 mediates cell-to-cell signaling during Arabidopsis stomatal development. *Plant Cell* **14**, 1527-1539.

Yang, M. and Sack, F. D. (1995). The *too many mouths* and *four lips* mutations affect stomatal production in Arabidopsis. *Plant Cell* **7**, 2227-2239.

Zhang, Y., Wang, P., Shao, W., Zhu, J.-K. and Dong, J. (2015). The BASL polarity protein controls a MAPK signaling feedback loop in asymmetric cell division. *Dev. Cell* **33**, 136-149.

Zhao, Y., Chow, T. F., Puckrin, R. S., Alfred, S. E., Korir, A. K., Larive, C. K. and Cutler, S. R. (2007). Chemical genetic interrogation of natural variation uncovers a molecule that is glycoactive. *Nat. Chem. Biol.* **3**, 716-721.
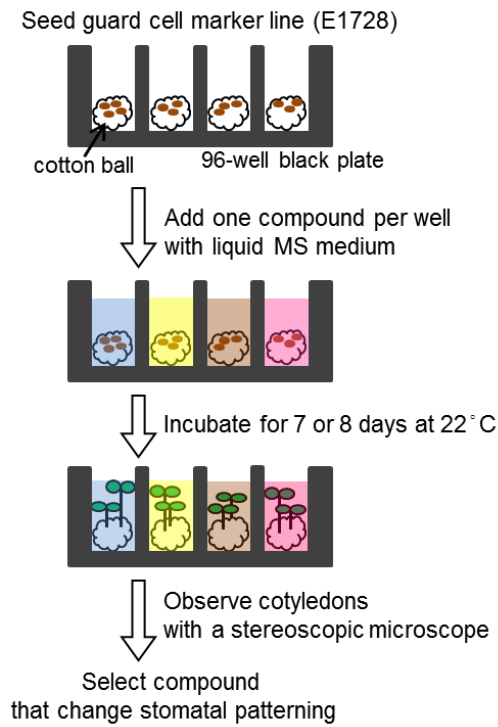
DEVELOPMENT

Fig. S1. The high-throughput chemical screening system.
Schematic representation of the high-throughput screening system
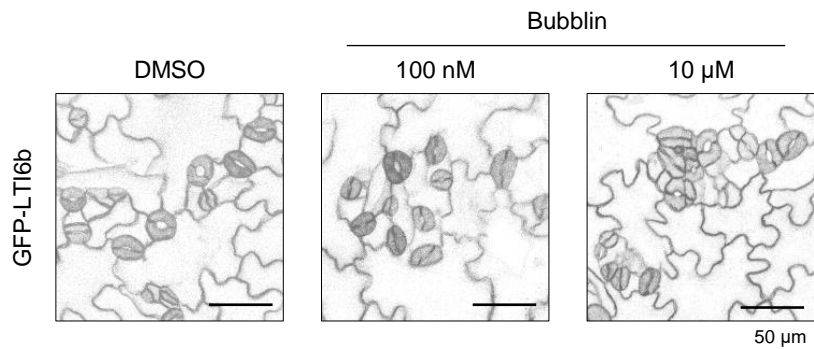used to identify compounds that affect stomatal patterning.

Fig. S2. 100 nM bubblin does not affect stomatal development. Confocal images of abaxial cotyledon epidermis from 10-day-old GFP-LTI6b seedlings treated with DMSO only as a control, 100 nM bubblin, or 10 µM bubblin.
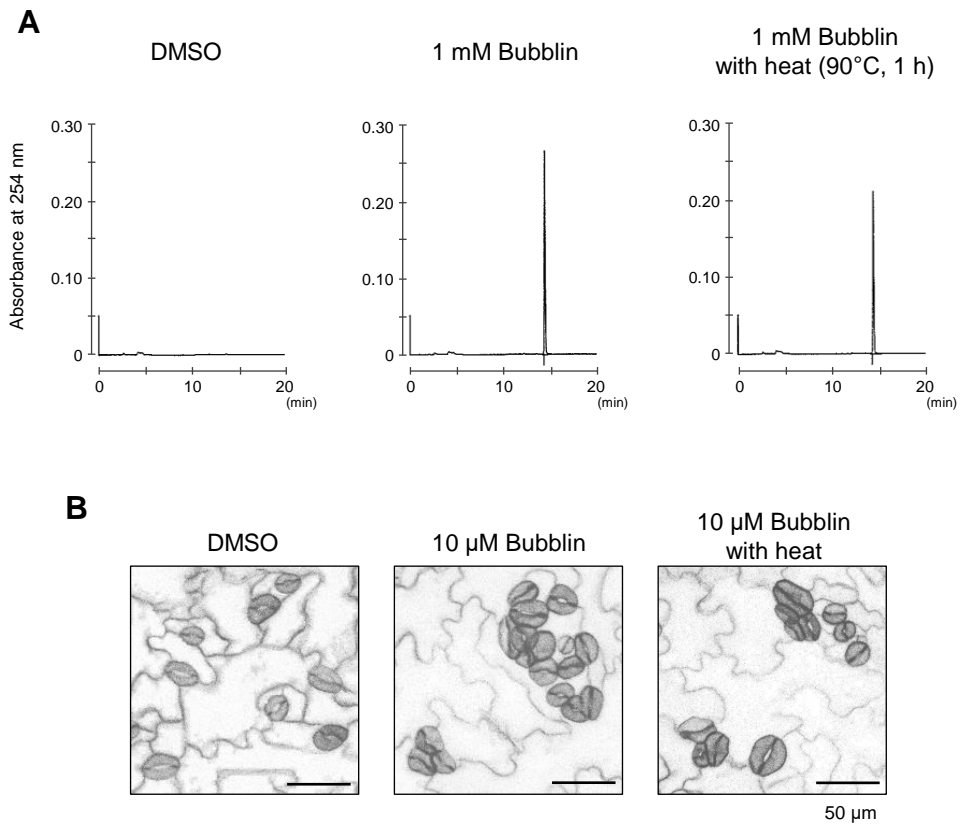
A

B

Fig. S3. Bubblin is not degraded and retains stomatal clustering activity after heat treatment. (A) Analytical HPLC profiles of DMSO, 1 mM bubblin, and 1 mM bubblin heated at 90° C for 1 h. (B) Confocal images of abaxial cotyledon epidermis from 10-day-old GFP-LTI6b seedlings treated with DMSO, 10 μM bubblin, or 10 μM bubblin heated at 90° C for 1 h.
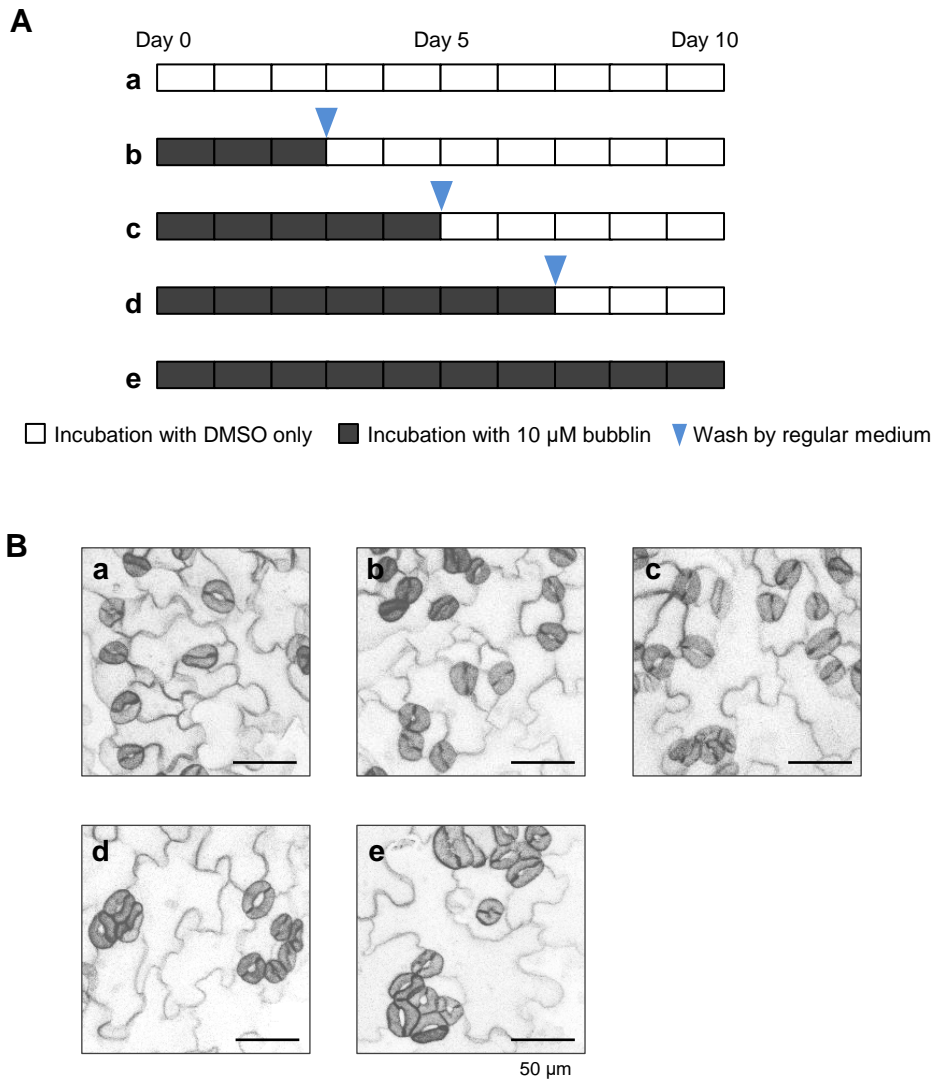
Fig. S4. Time-dependent effect of bubblin. (A) Rescue treatments used for
data presented in (B). Bubblin-treated seedlings were transferred to regular
medium at the indicated time points. Black boxes indicate the presence of
bubblin, white boxes indicate the number of days in regular medium, and blue
arrow heads indicate the day when seedlings were washed and transferred. (B)
Confocal images of abaxial cotyledon epidermis from 10-day-old GFP-LTI6b
seedlings treated with 10 μM bubblin for each time period indicated in (A).
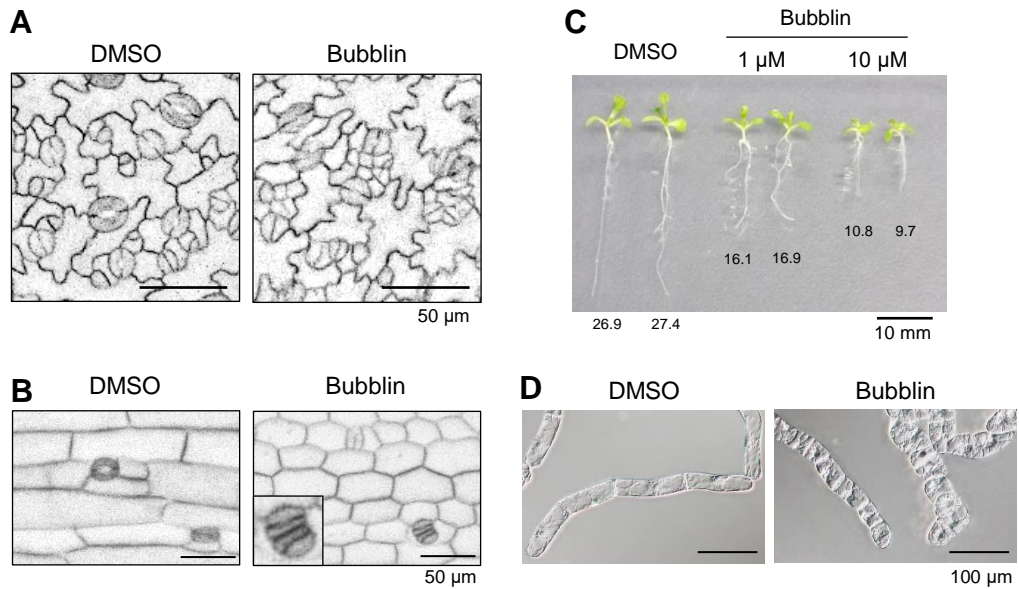
Fig. S5. Bubblin induces stomatal clustering in various tissues, and broadly affects cell size. (A) Confocal images of first leaves from 10-day-old GFP-LTI6b seedlings treated with DMSO or 10 μM bubblin. (B) Confocal images of hypocotyls from 10-day-old GFP-LTI6b seedlings treated with DMSO or 10 μM bubblin. A inset shows a magnified stomatal cluster. (C) Whole 10-day-old plants treated with DMSO, 1 μM bubblin, or 10 μM bubblin. Root lengths (mm) are indicated under each seedling. (D) Tobacco BY-2 cultured cells treated with DMSO or 10 μM bubblin for 3 days.
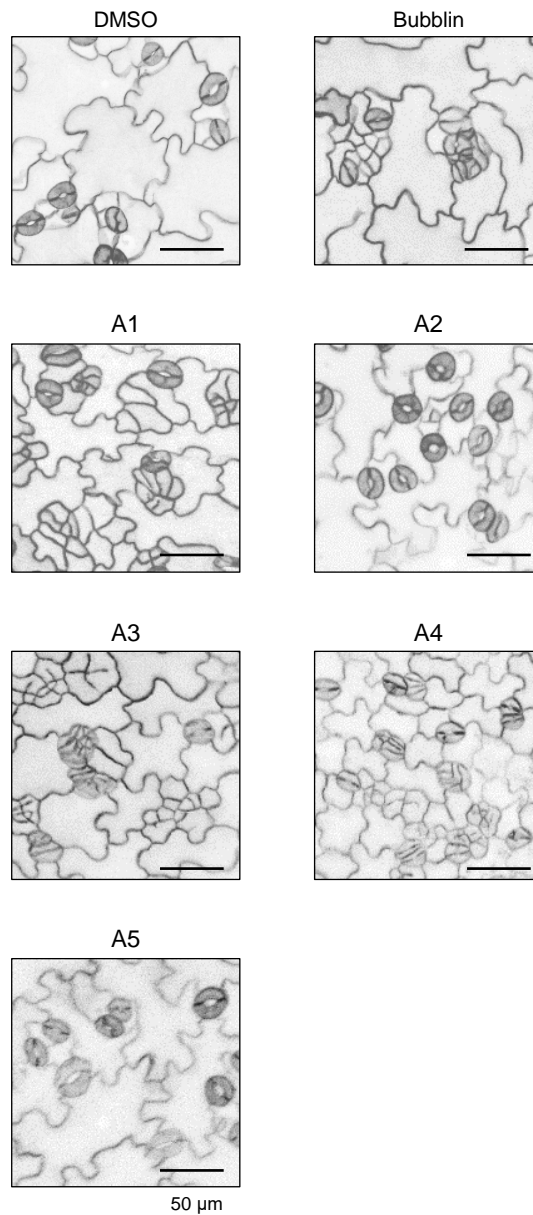
Fig. S6. Effect of 50 μM bubblin and five derivatives on stomatal patterning. Confocal images of abaxial cotyledon epidermis from 10-day-old GFP-LTI6b seedlings treated with the indicated compounds at 50 μM.

A

B
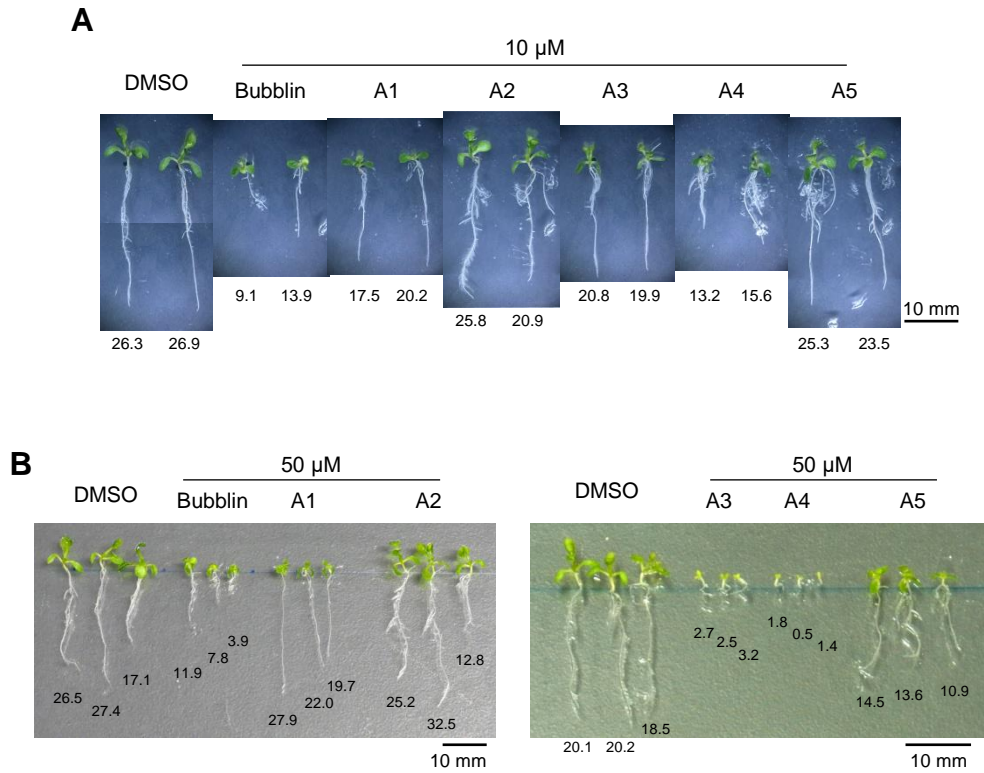
Fig. S7. The effect of five bubblin derivatives on seedling growth.
Whole 10-day-old plants treated with the derivatives A1 to A5 at 10 µM
(A) or 50 µM (B). Root lengths (mm) are indicated under each seedling.
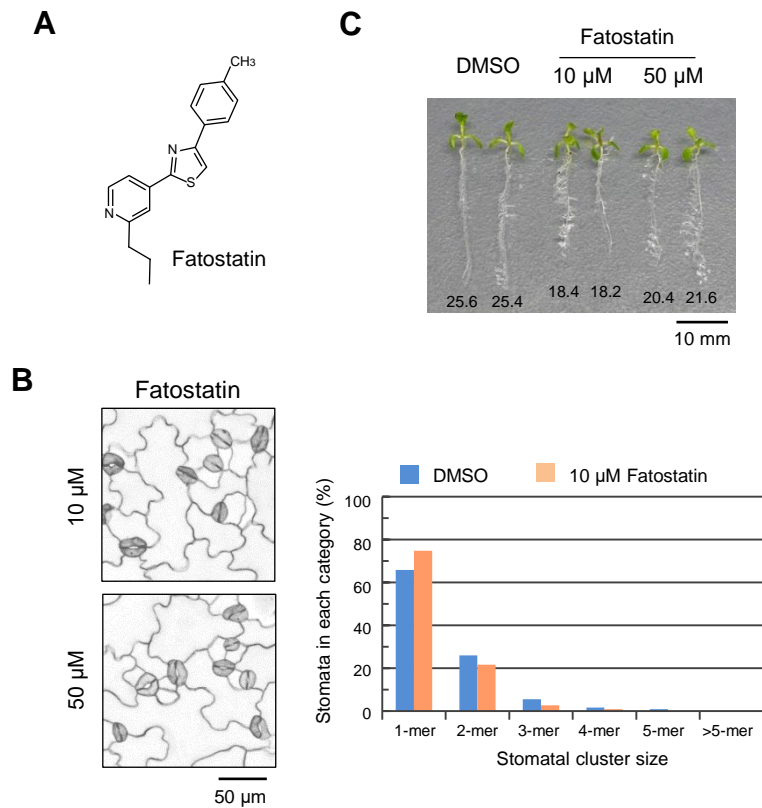
Fig. S8. Fatostatin has no effect on stomatal development or seedling growth.
(A) Chemical structure of fatostatin. (B) Confocal images of abaxial cotyledon epidermis from 10-day-old GFP-LTI6b seedlings treated with 10 μM or 50 μM fatostatin. Quantitative analysis indicates that fatostatin has no stomatal clustering activity. The percentage of stomata in each cluster size class is shown. Stomata (*n* = 485 (DMSO), *n* = 443 (10 μM fatostatin)) from 10 independent observations were counted for each treatment. (C) Whole 10-day-old plants treated with DMSO, 10 μM fatostatin, or 50 μM fatostatin. Root lengths (mm) are indicated under each seedling.

DMSO   Bubblin

50 µm
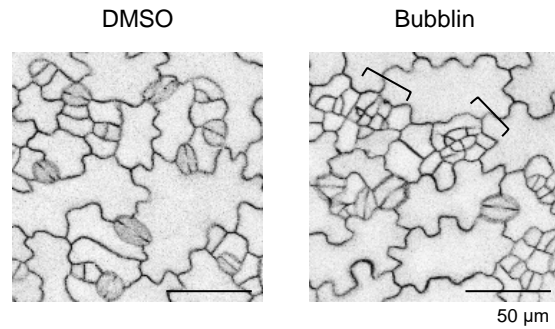
Fig. S9. Bubblin generates clustered small cells.
Confocal images of abaxial cotyledon epidermis from 7-
day-old GFP-LTI6b seedlings treated with DMSO or 10
µM bubblin. Bubblin-induced small cell clusters are
indicated by brackets.
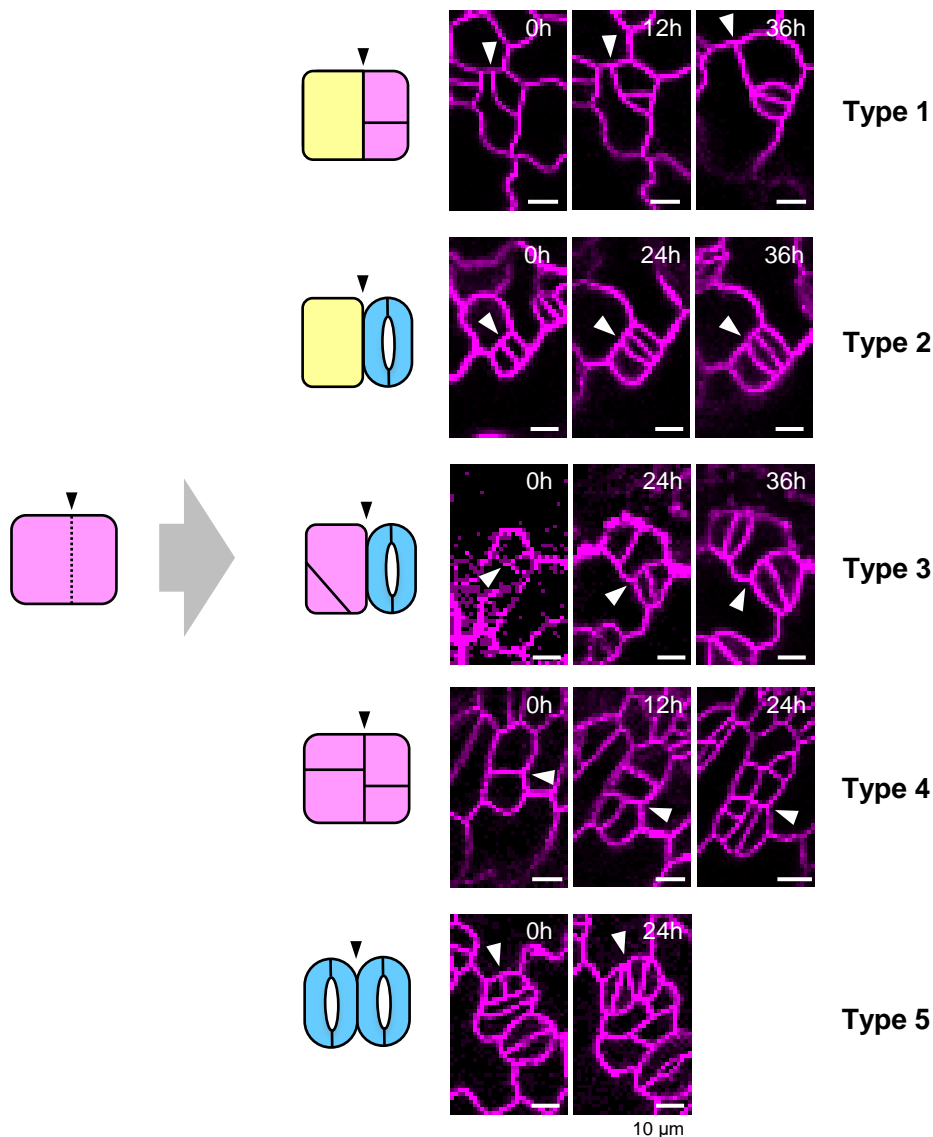
Fig. S10. Five types of divisions exhibited by stomatal lineage cells. Confocal images showing representative divisions categorized into types 1 to 5. Arrowheads indicate the planes of division that were categorized. Divisions of types 1 to 3 produce two daughter cells with different cell fates: type 1 produces a continuously dividing stomatal stem cell (magenta) and an expanding pavement cell (yellow), type 2 results in a pavement cell and a stoma that is composed of a pair of guard cells (blue), and type 3 generates a stoma and a stomatal stem cell. Divisions that produce daughter cells with the same cell fate are categorized into type 4 and type 5: type 4 divisions result in adjacent stomatal stem cells and type 5 divisions result in paired stomata.

A

Meristemoid   GMC   GC

SPCH   MUTE   FAMA

B

DMSO   Bubblin

EPF2-ox

EPF1-ox

50 µm
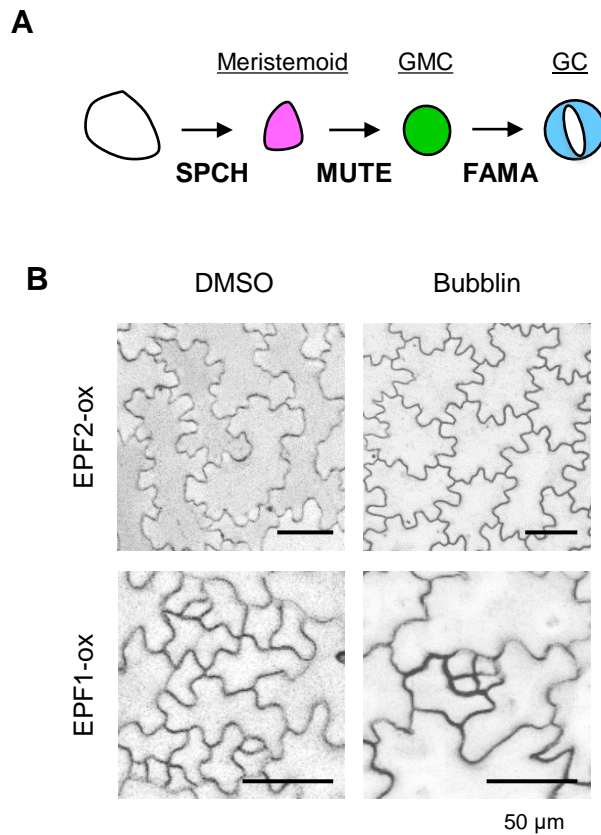
Fig. S11. Effect of bubblin on *EPF*-overexpressors.
(A) Three paralogous bHLH transcription factors (SPCH,
MUTE, and FAMA) regulating cell-fate transition during
stomatal development. (B) Confocal images of abaxial
cotyledon epidermis from 10-day-old EPF2-ox seedlings
and EPF1-ox seedlings treated with DMSO or 10 µM
bubblin.
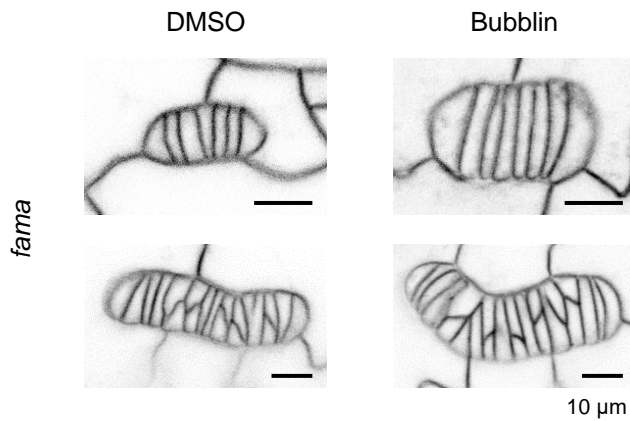
Fig. S12. Bubblin has no effect on the cells within *fama* tumors.
High-resolution images of *fama* tumors in 7-day-old cotyledon
epidermis treated with DMSO or 10 μM bubblin. There were no
significant differences in their dividing patterns between bubblin-
treated and mock-treated epidermis (upper). Some excessive divisions
in tumor cells were frequently observed in both conditions (lower).
Cell shape was visualized by FM4-64 dye staining.
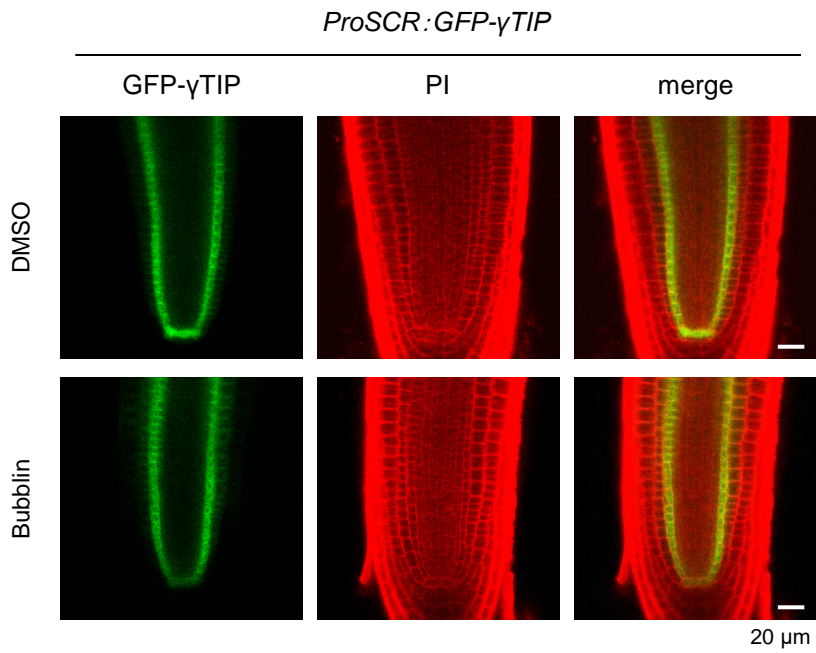
Fig. S13. Bubblin has no effect on asymmetric cell divisions in the root apical meristem. Confocal images of root tip from 8-day-old *ProSCR:GFP-γTIP* seedlings treated with DMSO or 10 μM bubblin. Endodermis is labeled by GFP. Cell shapes were visualized by PI staining.
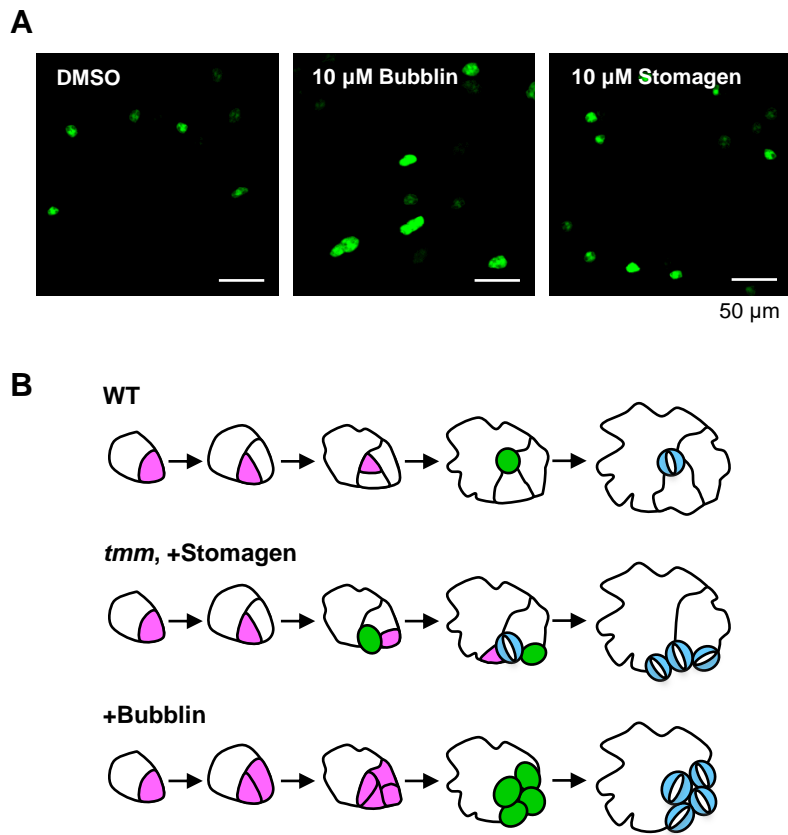
Fig. S14. Effect of bubblin on extrinsic mechanisms of stomatal patterning.
(A) Low-magnification confocal images of adaxial cotyledon epidermis from
6-day-old *ProSDD1:GFP* seedlings treated with DMSO, 10 μM bubblin, or 10
μM stomagen. (B) Schematic models of stomatal development in three
conditions (wild-type (WT), loss of TMM or stomagen treatment, and bubblin
treatment).
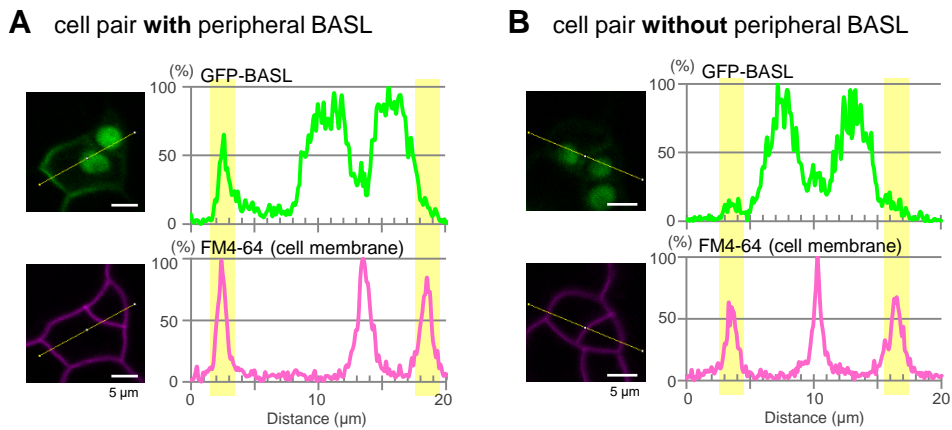
Fig. S15. The divided cell with or without peripheral BASL. (A, B) Left: confocal images of adaxial cotyledon epidermis from 6-day-old and 7-day-old *ProBASL:GFP-BASL* treated with DMSO (A) and with 10 μM bubblin (B), respectively. Cell shape was visualized by FM4-64 dye staining (magenta). Right: relative intensities of GFP-BASL and FM4-64 (cell membrane) were plotted along the lines indicated in the confocal images, with maximum luminance value set to 100%. Yellow bands highlight two distal cell membranes from the division plane between two daughter cells. The cell pair displayed in (A) maintains GFP-BASL signals in the cell periphery, but that in (B) does not maintain GFP-BASL signals in the cell periphery, and loses polarity.

A
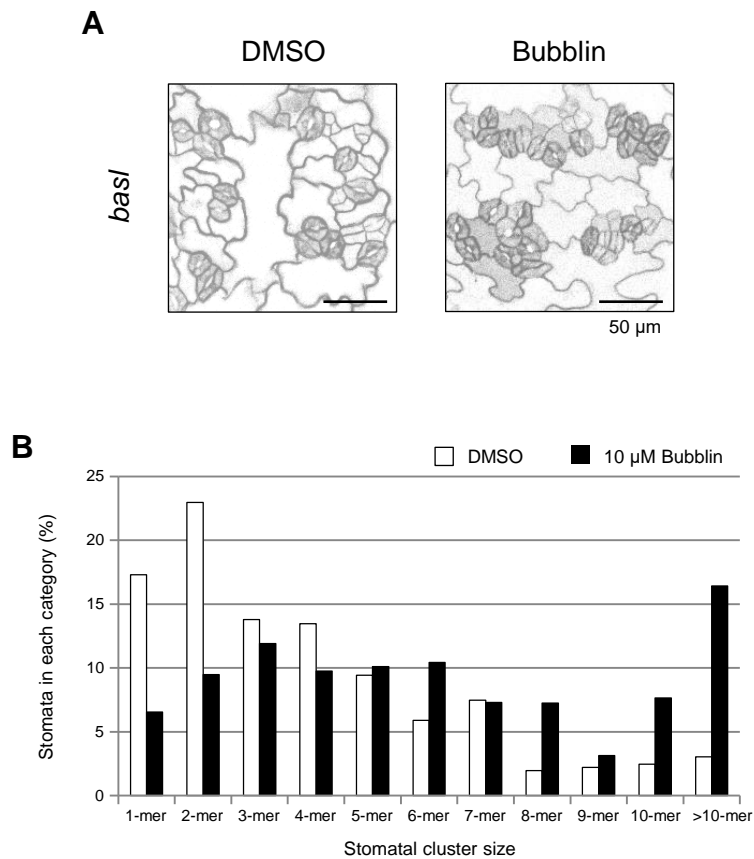
Fig. S16. Bubblin enhances the stomatal clustering phenotype in *basl*.
(A) Confocal images of abaxial cotyledon epidermis from 8-day-old *basl*
treated with DMSO or 10 μM bubblin. (B) Quantitative analysis of the
stomatal clustering displayed in (A). The percentage of stomata in each
cluster size class is shown. Stomata (*n* = 1219 (DMSO), *n* = 1436 (10 μM
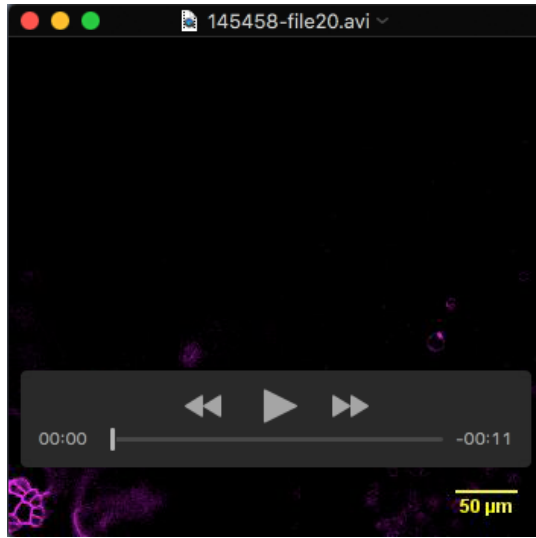bubblin)) from 16 independent observations were counted for each treatment.

Movies
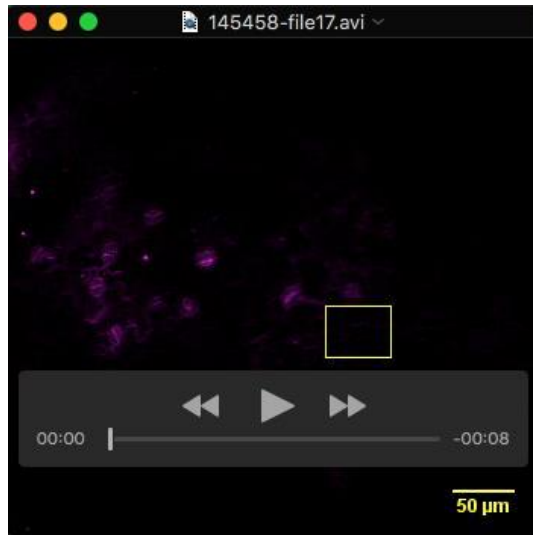
Movie 1. Z-stack series of full-size images of adaxial epidermis from DMSO-treated cotyledon at the experimental starting point (0 h, 4-day-old seedling). A yellow square indicates the area that is shown in Fig. 3A.
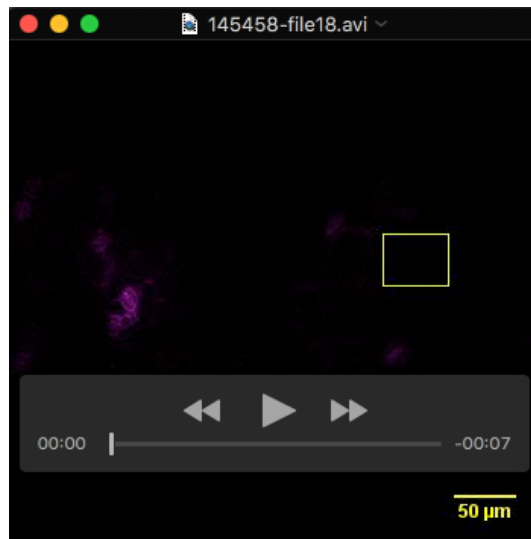
Movie 2. Z-stack series of full-size images of adaxial epidermis from DMSO-treated cotyledon at 12 h after initiation of treatment. A yellow square indicates the area that is shown in Fig. 3A.
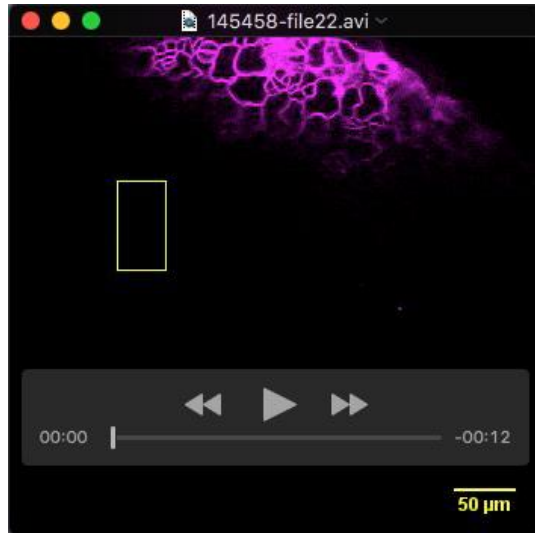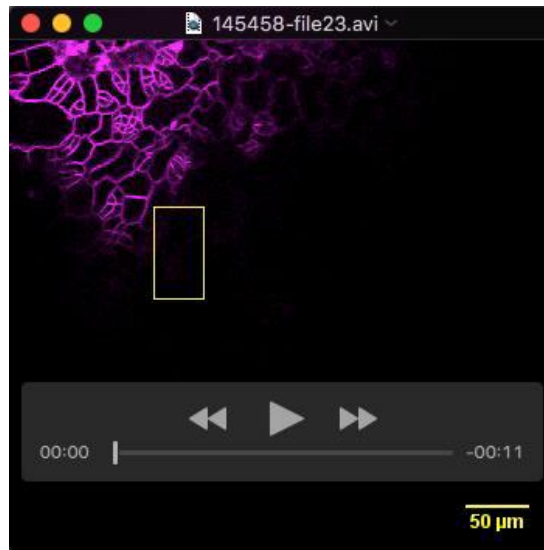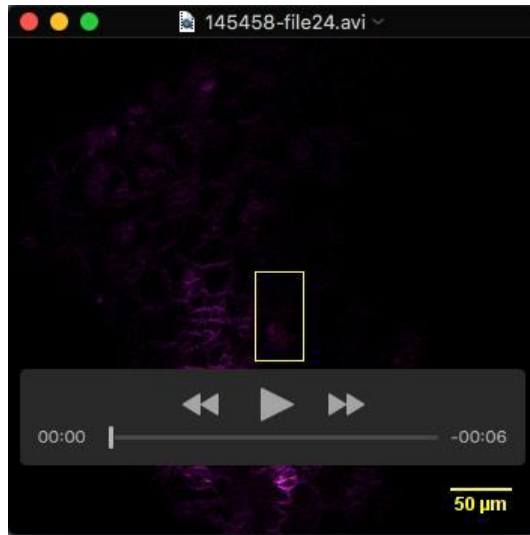
Movie 3. Z-stack series of full-size images of adaxial epidermis from DMSO-treated cotyledon at 24 h after initiation of treatment. A yellow square indicates the area that is shown in Fig. 3A.

Movie 4. Z-stack series of full-size images of adaxial epidermis from DMSO-treated cotyledon at 36 h after initiation of treatment. A yellow square indicates the area that is shown in Fig. 3A.

Movie 5. Z-stack series of full-size images of adaxial epidermis from bubblin-treated cotyledon at the experimental starting point (0 h, 4-day-old seedling). A yellow square indicates the area that is shown in Fig. 3B.

Movie 6. Z-stack series of full-size images of adaxial epidermis from bubblin-treated cotyledon at 12 h after initiation of treatment. A yellow square indicates the area that is shown in Fig. 3B.

Movie 7. Z-stack series of full-size images of adaxial epidermis from bubblin-treated cotyledon at 24 h after initiation of treatment. A yellow square indicates the area that is shown in Fig. 3B.

Movie 8. Z-stack series of full-size images of adaxial epidermis from bubblin-treated cotyledon at 36 h after initiation of treatment. A yellow square indicates the area that is shown in Fig. 3B.
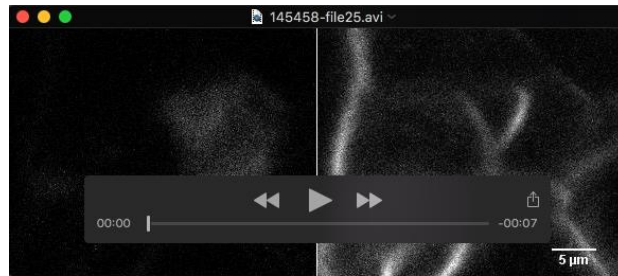
Movie 9. Z-stack series of adaxial cotyledon epidermis from *ProBASL:GFP-BASL* treated with DMSO only as a control. Left: GFP-BASL signal; right: FM4-64-stained cell membrane.
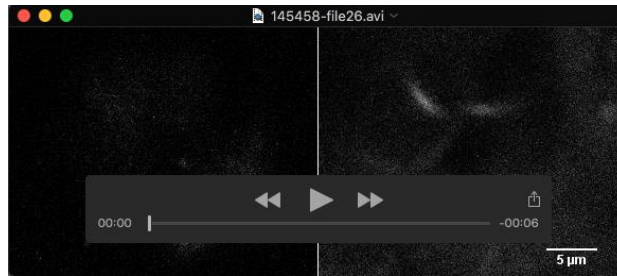
Movie 10. Z-stack series of adaxial cotyledon epidermis from *ProBASL:GFP-BASL* treated with 10 μM bubblin. Left: GFP-BASL signal; right: FM4-64-stained cell membrane.
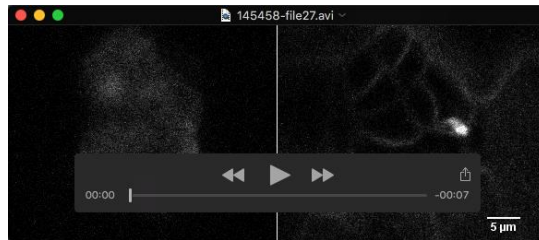
Movie 11. Z-stack series of adaxial cotyledon epidermis from *ProBASL:GFP-BASL* treated with 50 μM bubblin. Left: GFP-BASL signal; right: FM4-64-stained cell membrane.